doi:10.1246/cl.2011.1371
Published on the web November 26, 2011

Fast Synthesis of Highly Dispersed Anatase TiO_2 Nanocrystals in a Microfluidic Reactor

Li Zhang,[1] Yaogang Li,[2] Qinghong Zhang,*[2] Guoying Shi,[1] and Hongzhi Wang*[1]
[1]*State Key Laboratory for Modification of Chemical Fibers and Polymer Materials, Donghua University, Shanghai 201620, P. R. China*
[2]*Engineering Research Center of Advanced Glasses Manufacturing Technology, MOE, Donghua University, Shanghai 201620, P. R. China*

(Received August 22, 2011; CL-110706; E-mail: zhangqh@dhu.edu.cn)

An environmentally benign route has been developed to synthesize monodispersive anatase TiO_2 nanocrystals in organic solvent. The water-soluble peroxotitanium acid (PTA) was used as the precursor, which made the reaction practicable and facile in the microfluidic reactor. The perfectly crystallized anatase TiO_2 nanocrystals with a mean diameter of about 5.0 nm were obtained via a microfluidic reactor with a time as short as one or two minutes.

Titanium dioxide has attracted considerable attention for applications in dye-sensitized solar cells,[1] photocatalysts,[2] and components in electroceramics.[3] It is known that crystallized TiO_2 has three modification phases: anatase, rutile, and brookite, while the anatase phase displays the most efficient photocatalytic activity. Many methods have been established for the synthesis of nanostructured TiO_2 materials;[4] however, most of them need further annealing to induce the as-prepared TiO_2 transition from amorphous to anatase phase at higher temperature, which results in particle aggregation and reduces photocatalytic activity. Actually it is difficult to synthesize very small TiO_2 nanocrystals with a narrow size distribution and good crystallinity. There are too many oxygen vacancies and interstitial defects on the surface of quantum-sized TiO_2 nanocrystals, so the TiO_2 nanocrystals are prone to aggregate to reduce the high surface energies. Some people have used strongly coordinating organic capping agents to stabilize the TiO_2 nanocrystals, for example, An et al. prepared crystalline TiO_2 capped with oleic or stearic acid, which could be dispersed readily in toluene;[5] Li et al. synthesized monodispersed anatase TiO_2 nanoparticles using oleic acid as the surfactant and studied the roles of organic coating in tuning the defect chemistry of monodispersed TiO_2 nanocrystals for tailored properties.[6] However, the strongly bonded surfactant they used makes the surface of the synthesized nanocrystals hydrophobic, while most applications are carried out in aqueous solution,[7] and it is also supposed that the strongly bonded surfactant should passivate the surface activity of TiO_2 nanocrystals which has been thought to be correlated with its photovoltaic and photocatalytic properties.[8] Therefore, an alternative to develop synthetic methods to prepare phase-pure, small grain size, and highly crystallized TiO_2 not using strongly coordinating organic capping agents is urgently needed.

In the last decade, microfluidic technology has been widely used to synthesize nanocrystals because of excellent thermal conduction, rapid mixing speed, precise control of parameters, and superior physical stability.[9] In the microfluidic environment, the quantum-sized nanoparticles once formed would be enwrapped by the organic solvent and their further growth limited. Based on this idea, in this study, we obtained monodispersed anatase TiO_2 sol via the combination of microfluidic reactor with a mild water-soluble precursor PTA, which was appropriate to carry out in the microfluidic environment. The nanocrystals were formed within 2 min with hydroxy groups on the surface and uniformly dispersed in diethylene glycol (DEG) which has a very weak chelating ability.[10] It is demonstrated that the obtained monodispersed TiO_2 nanocrystals without using strongly coordinating organic capping agent would be useful for various applications including photocatalysis.

The PTA solution was lab-prepared according to previous work reported (Supporting Information[16]).[11] Typically, it was obtained by dissolving hydrous titania precipitates in the presence of H_2O_2, where the precipitates arose from the hydrolysis of titanium sulfate. The PTA solution was then dissolved in DEG with volume ratio 2:58 under stirring for an hour to form a clear solution and encased in a glass syringe. The solutions then were injected in a microcapillary (300 μm diameter, made of poly(tetrafluoroethylene) (PTFE), without any further inner surface treatment) by a syringe push pump and heated to 180 °C in oil bath for less than 2 min. Finally a small bottle was used to collect the products. The residence time of solution in microcapillary could be calculated by the driving speed, the diameter, and length of the microcapillary. To further characterize the particles in the sol, the obtained suspension (about 20 mL) was diluted with 160 mL of acetone to precipitate the particles. The particles were separated from the suspension by centrifuging at a speed of 8000 rpm for 10 min. The particles were dispersed in acetone and centrifuged for five more times to remove residual DEG and other impurities. The obtained solid particles were redispersed and stored in 20 mL of deionized water or alcohol for some characterization.

Transmission electron microscope (TEM) images and high-resolution TEM images were obtained using a JEM-2100 F TEM (JEOL Tokyo Japan) operating at 200 kV. Raman spectra were collected on a Fourier transform infrared–Raman spectrometer (NEXUS-5670, Nicolet, USA). The porous properties of samples were investigated using physical adsorption of N_2 at liquid-nitrogen temperature on an automatic volumetric sorption analyzer Autosorb-1 MP (Quantachrom SI, USA). Prior to measurement, the samples were degassed at 150 °C for 10 h. The specific surface area was determined according to the Brunauer–Emmett–Teller (BET) method, and the micropore size distributions were obtained by analysis of the adsorption branch of the isotherm by density functional theory (DFT). Elemental analysis (CHN) of the TiO_2 nanoparticles was carried out using a CHN analyzer (Vario EL III, Elementar, Germany).

As shown in Figure 1a, monodispersed TiO_2 nanocrystals with an average diameter of 5.0 nm are observed. The sample was redispersed in deionized water. From the HRTEM image

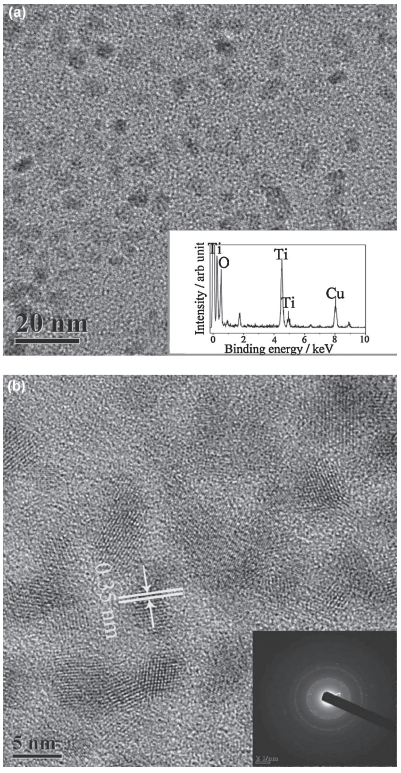

Figure 1. TEM and HRTEM images of TiO_2 nanocrystals dispersed in deionized water. (a) Low-magnification TEM and EDS spectrum images (inset), (b) high-resolution TEM image and SAED pattern (inset) of TiO_2 nanocrystals.

(Figure 1b), spherical TiO_2 nanocrystals with fringe spacing of 0.35 nm corresponding to (101) facets of anatase are observed. The clear fringe indicates that TiO_2 nanoparticles possess perfect crystallinity. The SAED pattern is consistent with the tetragonal structure of anatase TiO_2, with strong ring patterns being assigned to (101), (004), and (200) planes of anatase (Figure 1b, inset). EDS results indicate that the sample mainly consists of Ti, C, Cu, and O elements (Figure 1a, inset), and the C and Cu originated from the C-coated copper grid for TEM analysis. The carbon content of the TiO_2 nanoparticles is 0.054 wt % detected by CHN elemental analysis.

The crystallite size of anatase TiO_2 is very sensitive to the Raman signals. The dried TiO_2 sol shows major Raman bands of anatase TiO_2 at 151, 285, 398, 515, and 639 cm^{-1} (Figure 2), which can be attributed to the Raman-active modes of anatase phase with the symmetries of E_g, E_g, B_{1g}, A_{1g}, and E_g, respectively.[12] Compared to the E_g mode of bulk anatase TiO_2 at 143 cm^{-1}, the frequency shift observed is about 8 cm^{-1} of the strongest peak at 151 cm^{-1}. The shift of E_g to higher frequency is characteristic of anatase TiO_2 nanocrystals in the ultrafine size.[13] It shows that it is appropriate for the synthesis of anatase TiO_2 powder with a high degree of crystallinity and in ultrafine size in the microfluidic environment.

N_2 adsorption–desorption isotherms and calculated pore size distribution curves based on the density functional theory (DFT) of the TiO_2 particles are shown in Figure 3. The sample shows similar type-IV and type-I isotherms. In the very low relative pressure region ($P/P_0 < 0.01$), there is a large and steep rise in

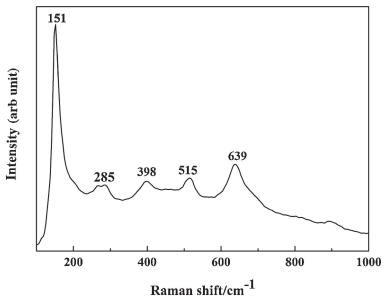

Figure 2. FT-Raman spectra of the dried TiO_2 sol.

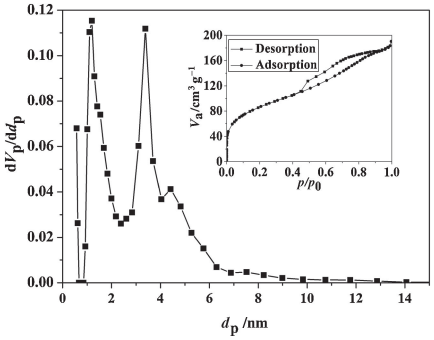

Figure 3. The pore-size distribution and N_2 adsorption–desorption isotherms (inset) of the dried TiO_2 sol.

the adsorption curve because of the sequential padding of the micropores. In the low and medium relative pressure regions ($0.01 < P/P_0 < 0.6$), they are monolayer and multilayer sorption, respectively. In the high relative pressure region ($P/P_0 > 0.6$), there is the capillary condensation with an increased adsorption volume growth reflected in Figure 3. The hysteresis loop is assigned to the presence of well-developed mesopores in the TiO_2 powders, and we estimate that the mesopore is shaped like a bottle-neck from the shape of the hysteresis loop. The DFT approach used to determine the mesopore size has fundamental advantages over the classical BJH method.[14] Here, using the DFT method, we find that bimodal pore size distributions exist in the dried TiO_2 sol, 1.5 and 3.5 nm, which is in accordance with the size of 1.3 nm calculated based on BJH theory from the desorption branch of the isotherm. The specific surface area and pore volume of the dried TiO_2 sol are 314.5 $m^2 g^{-1}$ and 0.27 $cm^3 g^{-1}$, also indicating the mean crystallite size of 5.0 nm, in accordance with the results observed in the TEM image (Figure 1b).

Microfluidic reactors have an increasingly important role in the synthesis of nanoparticles as an ideal medium.[9] A typical synthesis scheme for colloidal nanocrystals, including the burst of initial seeds, which occurs at a high temperature in the nucleation step and the growth of nuclei at a lower temperature in the reaction medium, has been adopted in the present work. After the PTA was injected from the syringe into a microcapillary in an oil-bath at 180 °C, the reaction began and initial TiO_2 seeds appeared. Then the seeds grew by residual heat while flowing to the end of the microcapillary. The nucleation and growth time are limited to 2 and 1 min in our experiment, respectively. It is conceivable that both the nucleation and the growth of nuclei could be controlled since the residence time

of the TiO_2 in the microcapillary is tunable. As the reaction continues, the abundant OH ligands existing in the PTA complex subsequently envelope the TiO_2 nuclei, which makes the TiO_2 nuclei highly dispersed in DEG. The TiO_2 enveloped by OH ligands may also emerge as promising filler material used for designing tissue engineered constructs (composite scaffolds) based on degradable polymer matrices.[15]

To verify the function of the microfluidic reactor in producing such spherical nanocrystals, a solution identical to the one for microfluidic reactor was directly injected into a Teflon-lined autoclave and then subjected to hydrothermal treatment. As clearly shown in Supporting Information,[16] irregular nanorod-like shapes with a broad range of sizes were obtained. The difference in morphology can probably be ascribed to the different hydrolysis behaviors of PTA under dissimilar conditions. During the microfluidic reactor treating process, PTA hydrolyzed as the solution was heated at 180 °C, followed by TiO_2 spheres enveloped by OH ligands. The residence time of 2 min in microcapillary restrained the further growth of the TiO_2 nanocrystals. In comparison, when the same solution was injected into a Teflon-lined autoclave for 4 h without undergoing microfluidic reaction, the PTA quickly hydrolyzed in the presence of water at a high temperature. Because hydrolysis and condensation proceeded simultaneously and very quickly, irregular nanorod-like shapes appeared as a result of uncontrolled attachment of TiO_2 nanoparticles. The nanorod-like TiO_2 nanoparticles were about 40 nm in length with the specific surface area of 150 $m^2 g^{-1}$, which is much smaller than the spherical TiO_2 nanocrystals (314.5 $m^2 g^{-1}$).

In summary, highly dispersed colloidal anatase TiO_2 nanocrystals have been successfully synthesized in a microfluidic reactor with a water-soluble precursor. Porous nanoparticles of approximately 5.0 nm with nearly spherical morphology could be well dispersed in DEG, which forms transparent colloidal solutions. Accordingly, it is demonstrated that the present microfluidic reactor approach could provide the TiO_2 sol with a high uniformity of physical and chemical properties.

The author thanks the Ministry of Education of China (No. 708039 and No. 111-2-04) and Shanghai Municipal Education Commission (No. 07SG37) for financial support.

References and Notes

1 a) B. O'Regan, M. Grätzel, *Nature* **1991**, *353*, 737. b) J. Jiu, S. Isoda, F. Wang, M. Adachi, *J. Phys. Chem. B* **2006**, *110*, 2087.
2 H. Irie, Y. Watanabe, K. Hashimoto, *Chem. Lett.* **2003**, *32*, 772.
3 U. Diebold, *Surf. Sci. Rep.* **2003**, *48*, 53.
4 a) X. Yang, H. Konishi, H. Xu, M. Wu, *Eur. J. Inorg. Chem.* **2006**, 2229. b) H. Uchiyama, K. Matsumoto, H. Kozuka, *Chem. Lett.* **2010**, *39*, 445.
5 D. Pan, N. Zhao, Q. Wang, S. Jiang, X. Ji, L. An, *Adv. Mater.* **2005**, *17*, 1991.
6 L. Li, G. Li, J. Xu, J. Zheng, W. Tong, W. Hu, *Phys. Chem. Chem. Phys.* **2010**, *12*, 10857.
7 S. Sakthivel, H. Kisch, *Angew. Chem., Int. Ed.* **2003**, *42*, 4908.
8 a) T. L. Thompson, J. T. Yates, Jr., *Chem. Rev.* **2006**, *106*, 4428. b) P. Wang, D. Wang, H. Li, T. Xie, H. Wang, Z. Du, *J. Colloid Interface Sci.* **2007**, *314*, 337.
9 a) X. Zhu, Q. Zhang, Y. Li, H. Wang, *J. Mater. Chem.* **2008**, *18*, 5060. b) H. Nakamura, A. Tashiro, Y. Yamaguchi, M. Miyazaki, T. Watari, H. Shimizu, H. Maeda, *Lab Chip* **2004**, *4*, 237. c) B. F. Cottam, S. Krishnadasan, A. J. deMello, J. C. deMello, M. S. P. Shaffer, *Lab Chip* **2007**, *7*, 167. d) H. Wang, H. Nakamura, M. Uehara, M. Miyazaki, H. Maeda, *Chem. Commun.* **2002**, 1462.
10 X. Jiang, T. Herricks, Y. Xia, *Adv. Mater.* **2003**, *15*, 1205.
11 S. Li, Y. Li, H. Wang, W. Fan, Q. Zhang, *Eur. J. Inorg. Chem.* **2009**, 4078.
12 T. Ohsaka, F. Izumi, Y. Fujiki, *J. Raman Spectrosc.* **1978**, *7*, 321.
13 S. Kelly, F. H. Pollak, M. Tomkiewicz, *J. Phys. Chem. B* **1997**, *101*, 2730.
14 B. Smarsly, S. Polarz, M. Antonietti, *J. Phys. Chem. B* **2001**, *105*, 10473.
15 L.-C. Gerhardt, G. M. R. Jell, A. R. Boccaccini, *J. Mater. Sci.: Mater. Med.* **2007**, *18*, 1287.
16 Supporting Information is available electronically on the CSJ-Journal Web site, http://www.csj.jp/journals/chem-lett/index.html.

